Nature of the effective interaction in electron-doped cuprate superconductors: A sign-problem-free quantum Monte Carlo study

Zi-Xiang Li, Fa Wang, Hong Yao, and Dung-Hai Lee

The nature of effective interaction in electron-doped cuprate superconductors: a sign-problem-free quantum Monte-Carlo study

Zi-Xiang Li[1], Fa Wang[2,3], Hong Yao[1,3], and Dung-Hai Lee[4,5]

[1] *Institute for Advanced Study, Tsinghua University, Beijing 100084, China.*
[2] *International Center for Quantum Materials, School of Physics, Peking University, Beijing 100871, China.*
[3] *Collaborative Innovation Center of Quantum Matter, Beijing, China.*
[4] *Department of Physics, University of California, Berkeley, CA 94720, USA.*
[5] *Materials Sciences Division, Lawrence Berkeley National Laboratory, Berkeley, CA 94720, USA.*

Understanding the mechanism of Cooper pairing amounts to determining the effective interaction that operates at low energies. Achieving such a goal for superconducting materials, especially strongly correlated ones, from both bottom-up and top-down approaches have been plagued with having to use uncontrolled approximations. Here, we perform large-scale, numerically-exact, sign-problem-free, zero-temperature quantum Monte-Carlo simulations on an effective theory based on "hot spots" plus fluctuating collective modes. Because hot spots are clearly identified by angle-resolved photoemission spectroscopy for *electron-doped* cuprates we focus our attention to such materials. Our goal is to determine the minimum effective action which can describe the observed superconductivity and charge density wave. The results suggest that antiferromagnetic fluctuation alone is *not sufficient* – the effective action needs to be amended with nematic fluctuations. We believe our results address the pairing mechanism of high T_c superconductivity in electron-doped cuprates and shed light on that of hole doped cuprates.

Thirty years after the discovery of the cuprate high temperature superconductors[1] a consensus on the pairing mechanism is yet to be reached. The main obstacle are two folds. (1) The theoretical methods used to address this problem are not free from uncontrolled approximations. (2) In addition to high temperature superconductivity there are a number of "companion instabilities" begging for a unified explanation.

In the last few years it is established that in addition to the antiferromagnetic (AFM) and superconducting (SC) instabilities both electron and hole doped cuprates superconductors exhibit the propensity toward charge density wave (CDW) order[2–12, 14]. These instabilities together with nematicity[15–18] form the so-called "intertwined orders" of the cuprate superconductors[19–21]. Finding the correct effective interaction to explain all these instabilities is in high demand.

In the absence of controlled bottom-up theory, phenomenological approaches based on the assumption that AFM fluctuation is responsible for the plethora of electronic instabilities have been quite useful[20–27]. However, like other cuprate theories, these approaches involve approximations that can not be *a priori* justified.

In this paper we focus on *electron doped* cuprates where angle resolved photoemission spectrocopy (ARPES)[28, 29] clearly show spectral weight suppression near the hot spots (Fig.(1a)) as opposed to near the "antinodes" for hole doped cuprates. Such suppression has been interpreted as the scattering of fermion excitations by AFM collective modes[30]. In addition it was found that in the superconducting state, the gap peaks around the hot spots[31, 32]. This motivates an effective theory which retains the fermionic excitations near the hot spots and couple them to the fluctuating AFM collective

modes. Such effective theory has been used to address the AFM quantum phase transition[33–36]. In 2012 Berg *et al.*[37] utilized a generalized time reversal symmetry to achieved a sign-problem-free finite temperature quantum Monte-Carlo simulation on a *two-band* model featuring the AFM fluctuations and hot spots similar to the cuprates (Fig. 1(b)). Their results suggest that quantum critical AFM fluctuation enhances SC pair correlations in the *d*-wave channel (although the *d*-wave long-range order has not be numerically observed).

Like the hole doped cuprates, CDW correlation has been observed in electron doped $Nd_{2-x}Ce_xCuO_4$[12, 13]. Moreover the CDW occurs in the region of phase diagram where the AFM fluctuation is expected to be strong. Remarkbly this CDW has similar ordering wavevectors as those of the hole doped cuprates (although the CDW amplitude is apparently much weaker). This motivates us to investigate whether the hot spots plus AFM fluctuations can also account for the observed CDW.

We perform large-scale, sign-problem-free, zero-temperature projector QMC simulations[38–40] to answer this question (see the details of projector in [41]). The main results are summarized as follows. (1) When there is only AFM fluctuations we obtain the phase diagram in Fig.1(d), which shows the AFM, SC and the AFM-SC coexistence phases. (2) For a wide range of parameters we found AFM fluctuations can trigger *d*-wave superconducting *long-range order.* Moreover the strongest SC occurs near the AFM quantum critical point. (3) However the CDW correlation triggered by the AFM fluctuations exhibit ordering wave vectors that are *inconsistent* with the observed ones. (4) We show that AFM plus nematic fluctuations predicts a CDW correlation with the correct ordering wavevectors. The phase
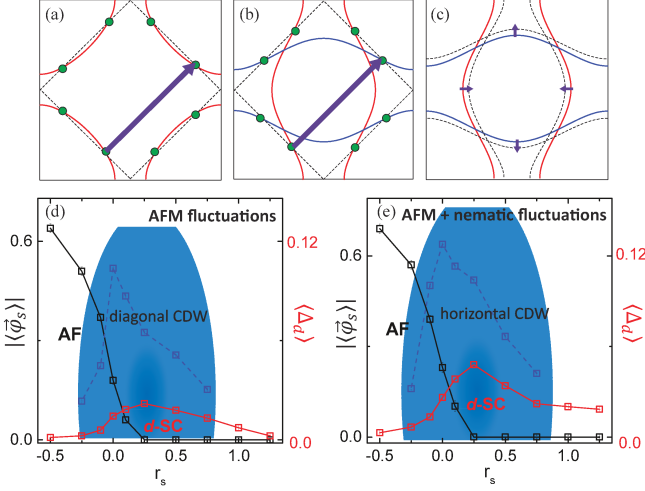
FIG. 1. (a) A prototypical Fermi surface of the cuprates. The dashed lines enclose the AFM Brillouin zone, the hot spots are denoted by the green dots and the purple arrow indicates the AFM ordering wavevector (π, π). (b) The Fermi surfaces of the two-band model where the positions of hot spots and the Fermi velocity at hot spots are made to mimic those in the single-band model used to describe the cuprates. The red/blue Fermi surfaces are derived from the bands formed by the x and y orbitals described by the action in Eq. (S1). (c) The nematically distorted Fermi surface. The arrows indicate the distortion. (d) AFM order parameter $|\langle \vec{\varphi_s} \rangle|$ and d-wave SC order parameter $\langle \Delta_d \rangle$ as a function of r_s. For each value of r_s we perform finite size extrapolation to determine the order parameters in the thermodynamic limit. The blue points represent the maximum d-wave bond CDW structure factor which is reached at the diagonal wavevectors for $L = 16$. (f) AFM order parameter $|\langle \vec{\varphi_s} \rangle|$ and d-wave SC order parameter $\langle \Delta_d \rangle$ as a function of r_s when both AFM and nematic fluctuations are considered. The blue points are the maximum d-wave bond CDW structure which is reached at the horizontal wavevectors for $L = 16$. It is remarkable that adding nematic fluctuation can not only enhance d-wave superconducting pairing but also induce the CDW wavevectors consistent with recent experiments[12].

diagram for this situation is shown in Fig. 1(e). (5) The resulting CDW is a stripe-like, d-form factor, bond density wave. (6) The nematic fluctuation enhances the d-wave superconductivity[46]. These results lead us to conclude that the an effective action featuring "hot spots" and both antiferromagnetic and nematic fluctuations describes the low energy physics of electron doped cuprates.

Following Ref. [37] we consider a two-band model where the bands are derived from two orbitals on each site of the square lattice. The Fermi surfaces (marked red and blue in Fig. 1(b)) of this model share nearly the same electronic structure near the hot spots (green dots) with the cuprates. This bandstructure is supplemented with the quantum Ginzburg-Landau action describing fluctuating AFM and nematic order parameters. Moreover, these order parameters couple to electrons by the

Yukawa coupling. The effective action is then given by

$$S = S_F + S_s,$$
$$S_F = \int_0^\beta d\tau \Big\{ \sum_{ij, \alpha = x, y} \psi_{i\alpha}^\dagger \big[(\partial_\tau - \mu) \delta_{ij} - t_{ij, \alpha} \big] \psi_{j\alpha}$$
$$+ \lambda_s \sum_i (-1)^i \big[\psi_{ix}^\dagger (\vec{\sigma} \cdot \vec{\varphi}_i) \psi_{iy} + h.c. \big] \Big\},$$
$$S_s = \int_0^\beta d\tau \Big\{ \frac{1}{2} \sum_i \frac{1}{c_s^2} |\partial_\tau \vec{\varphi}_i|^2 + \frac{1}{2} \sum_{\langle ij \rangle} |\vec{\varphi}_i - \vec{\varphi}_j|^2$$
$$+ \sum_i \Big[\frac{r_s}{2} |\vec{\varphi}_i|^2 + \frac{u_s}{4} \big(|\vec{\varphi}_i|^2 \big)^2 \Big] \Big\}. \tag{1}$$

Here i labels the sites of a square lattice, $\alpha = x, y$ labels the two orbitals (which transform into each other under the 90° rotation) from which the red and blue Fermi surfaces in Fig. 1(b) are derived from, τ denotes the imaginary time and β is the inverse temperature. In Eq. (1) $\vec{\varphi}$ is the Néel order parameter and the operator $\psi_{i\alpha}$ is a spinor operator which annihilates an electron in orbital α and on site i. The three $\vec{\sigma}$ are the spin Pauli matrices.

It is worth of noting that the model is purely phenomenological. We *assume* it captures the important low energy degrees of freedom of the electron doped cuprates. The goal is to check whether the prediction of such *effective theory* agrees with the observations by performing approximation-free computations. We stress that our goal is not to show such theory is the low energy effective theory of Hubbard or t-J type models. The parameters in this effective action include the spin wave velocity c_s, and r_s which tunes the system across the AFM phase transition, and u_s is the self-interactions of the $\vec{\phi}$ field, and λ_s is the "Yukawa" coupling between the electrons and the AF fluctuation. The hopping integral t_{ij} is chosen to be among nearest-neighbor sites and equal to $t_\parallel = 1.0$ for $x(y)$-orbital along $x(y)$ direction and $t_\perp = 0.5$ for $y(x)$ orbital along $x(y)$ direction. We choose the chemical potential to be $\mu = -0.5$ such that the Fermi surface is shown in Fig. 1(b).

Aside from the square lattice spatial symmetries the action is invariant under the anti-unitary transformation $U = i\tau_z \sigma_y K$, where τ_z is the third Pauli matrix acting in orbital space and K denotes complex conjugation. It can be shown that because of this symmetry, the fermion determinant for arbitrary $\vec{\varphi}_i(\tau)$ configuration is positive hence the QMC simulation is free of minus-sign. This enables us to perform large-scale projective QMC simulation. In the following we first focus on the pure AFM fluctuations.

The most important parameter in the AFM Ginzburg-Landau action is r_s which tunes the system across the order $(r_s < r_{s,c})$ – disorder $(r_s > r_{s,c})$ AFM quantum phase transition. Our large-scale projector QMC simulation is carried out on a square lattice with
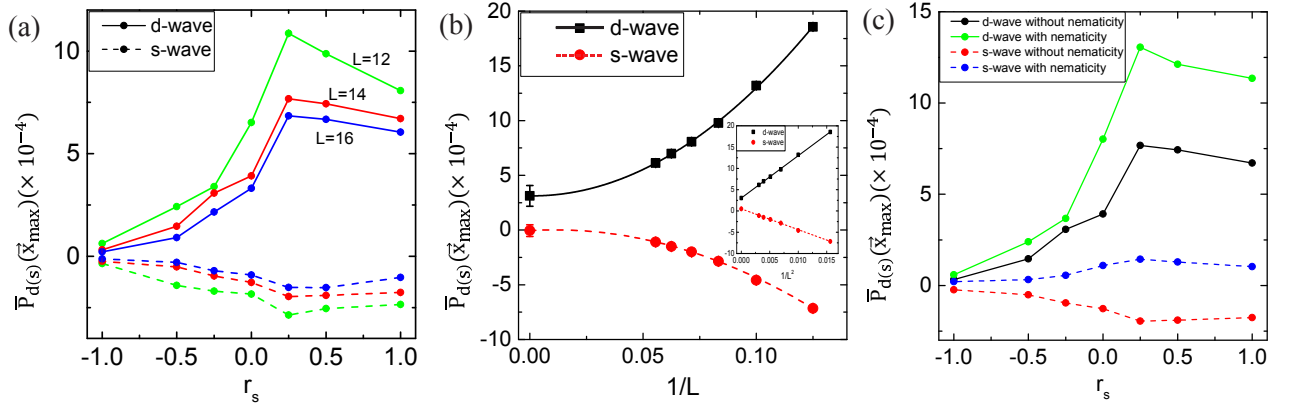
FIG. 2. (a) The s- and d-wave SC pair correlations $\overline{P}_{s/d}$ evaluated at maximum separation $\vec{x}_{\max} = (L/2, L/2)$ for $L = 12, 14, 16$ and various values of r_s. The peak of the enhancement for d-wave pairing occurs at $r_s \approx 0.25$ which is close to the AFM quantum critical point. (b) Both s- and d-wave pair correlations evaluated at $\vec{x}_{\max}$ are plotted versus $1/L$ for $L = 8, 10, 12, 14, 16, 18$. By fitting them using $f(1/L) = a + b/L + c/L^2$ and extrapolating to the thermodynamic limit ($L = \infty$), we find that the d-wave pairing correlations are extrapolated to a non-zero value, $(3.1 \pm 0.8) \times 10^{-4}$, while the s-wave pairing correlations to zero within the error bar. Interestingly the finite size dependence of both correlation functions are dominated by $1/L^2$ as shown by the nearly linear dependence of $\overline{P}_{d(s)}$ on $1/L^2$ in the inset of Fig. 2(b). These results clearly indicate that the ground state possesses d-wave superconducting long-range order. (c) The comparison of the d- and s-wave SC pairing correlations at $\vec{x}_{\max}$ in the system with $L = 14$, without and with nematic fluctuation. In the latter case, we set $r_n = 0.5$ which places the system on the disordered side of the nematic transition. The results show an considerably enhanced d-wave SC correlation by the nematic fluctuations.

$N = L \times L$ sites. Unless otherwise mentioned we use periodic boundary condition. From the finite-size scaling of the Binder-ratio[42] of the AFM order parameter, we determine $r_{s,c} \approx 0.25$ which is consistent with the value obtained in Ref. [37]. In the following we present the simulation results on the SC and CDW instabilities.

Cooper pairing induced by AFM fluctuations
To probe superconductivity we compute the equal-time pair-pair correlation function $\overline{P}_{d/s}(\vec{x}_{\max})$:

$$P_{s/d}(\vec{r}_i) = \langle \Delta_{s/d}(\vec{r}_i) \Delta_{s/d}^{\dagger}(\vec{0}) \rangle, \qquad (2)$$

where

$$\Delta_{s/d}(\vec{r}_i) = \psi_{ix}^T (i\sigma_y) \psi_{ix} \pm \psi_{iy}^T (i\sigma_y) \psi_{iy} \qquad (3)$$

are the s ($+$ sign) and d ($-$ sign) wave Cooper pair operators, respectively. We determine whether long-range superconducting order exists by examining the pair-pair correlation with pair fields separated by the maximum separation $\vec{x}_{\max} = (L/2, L/2)$. In addition, in order to minimize the statistical errors, we average $\vec{x}_{\max}$ over its nine nearest-neighbor values. Thus the actual pair correlation we study is $\overline{P}_{d(s)}(\vec{x}_{\max}) = \frac{1}{9} \sum_{n,m=0,\pm1} P_{d(s)}(\vec{x}_{\max} + n\hat{x} + m\hat{y})$ for the maximum spatial separation. Here s/d denotes s/d-wave pairing, respectively and $\vec{x}_{\max} = (L/2, L/2)$ is the maximum spatial separation between the pair fields for a system with linear dimension L. In Fig. 2(a) we plot $\overline{P}_{d/s}(L/2, L/2)$ for various system sizes L and different values of r_s. It clearly shows that the AFM spin fluctuation enhances d-wave pair correlation more than the s-wave. In particular

the enhancement for d-wave pairing is the strongest near the AFM quantum critical point $r_{s,c} \approx 0.25$.

To determine whether the ground state has SC long-range order we focus on $r_s = 0.5 > r_{s,c}$ and carefully study the size dependence of $\overline{P}_{d(s)}(L/2, L/2)$ for $L = 8, 10, 12, 14, 16, 18$. As shown in Fig. 2(b) the d-wave pair correlation function saturates to a non-zero value after extrapolating to $L = \infty$. (The red curve is the best fit using a quadratic polynomial of $1/L$). In contrast the s-wave pair correlation extrapolates to zero in the thermodynamic limit. These results clearly suggest that the ground state possesses d-wave SC *long-range order*.

In Fig. 1(d) we plot the expectation value of the AFM and d-wave SC order parameter as a function of r_s (we performed careful finite-size analysis for both order parameters at each r_s). Interestingly it is qualitatively similar to the finite temperature phase diagram of the electron doped cuprates. In particular our zero temperature result shows the coexistence of AFM and SC when these two phases overlap [47].

CDW correlation induced by AFM fluctuations
Recent resonant X-ray scattering experiments on eletron doped NCCO[12, 13] shows the existence of a stripe-like short-ranged CDW order with incommensurate ordering wavevectors approximately connecting neighboring hot spots. In this section we ask whether the AFM fluctuation can also trigger this CDW order. Two types of CDW order, namely the site and bond CDW, were studied. The
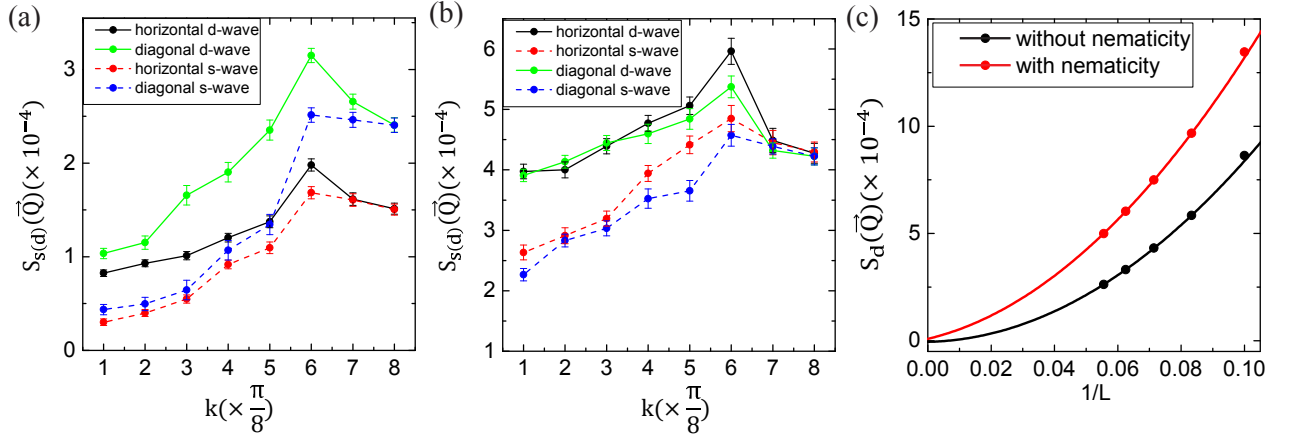
FIG. 3. (a) $\Delta S_{s/d}(\vec{Q})$, the difference between $S_{s/d}(\vec{Q})$ with ($r_s = 0.5$) and without the AF fluctuations, versus $\vec{Q}$ for $L = 16$. $S_{s/d}(\vec{Q})$ is the s- and d-wave bond CDW structure factor versus $\vec{Q} = (k, 0)$ (horizontal CDW) or $\vec{Q} = (k, k)$ (diagonal CDW). (b) $\Delta S_{s/d}(\vec{Q})$, the difference between $S_{s/d}(\vec{Q})$ with ($r_s = 0.5, r_n = 0.5$) and without the AFM+nematic fluctuations, for L=16. (c) $\Delta S_d(\vec{Q}_0)$ as a function of $1/L$ for $L = 14, 16, 18$. The red dots represent the enhancement of the peak d-wave bond CDW structure factor by both spin ($r_s = 0.5$) and nematic ($r_n = 0.5$) fluctuations. The black dots are the enhancement by spin fluctuations ($r_s = 0.5$) alone. The solid curves are the best fit using $f(1/L) = a + b/L + c/L^2$. In both cases the structure factors extrapolate to zero within error bar in the thermodynamic limit. It suggests that the bond CDW order induced by AFM and/or nematic fluctuations is short-ranged.

bond CDW operator is defined as:

$$B_{s/d}(i) = \sum_{a=\pm\hat{x}} \left[\psi_{ix}^{\dagger} \sigma_0 \psi_{i+a,x} + H.c. \right]$$
$$\pm \sum_{a=\pm\hat{y}} \left[\psi_{iy}^{\dagger} \sigma_0 \psi_{i+a,y} + H.c. \right], \quad (4)$$

where σ_0 is the identity 2×2 matrix and "+" sign corresponds to the s-wave and "−" to the d-wave formfactor, respectively. Under a $90°$ rotation around site i, $B_s(i) \to B_s(i)$ while $B_d(i) \to -B_d(i)$. Similarly, the site CDW operator is defined:

$$D_{s/d}(i) = \psi_{i,x}^{\dagger} \sigma_0 \psi_{i,x} + \psi_{iy}^{\dagger} \sigma_0 \psi_{iy} \quad (5)$$

We compute the structure factor of bond and CDW structure factor (see the definitions of CDW structure factors in [41]) and compare the strength of bond and site CDW in our effective model. The results show the bond CDW is favored [41]. Since whether the CDW has site or bond nature is open for electron doped cuprates[12] our result should be viewed as a *prediction*. For bond CDW we study structure factors with s and d symmetry form factors ($S_{s/d}(\vec{Q})$). When this quantity extrapolates to a non-zero value for a particular peak wavevector $\vec{Q}_0$ as $L \to \infty$, it signifies the existence of long-range CDW order with modulation period $2\pi/|\vec{Q}_0|$. Experimentally the strongest CDW modulation is observed for $\vec{Q}_0 = (\pm\delta, 0)$ and $(0, \pm\delta)$ in the Cu-Cu bond directions with $\delta \approx 2\pi/3$[12] which corresponds to a spatial period approximately three lattice constants.

In Fig. 3(a) we plot $\Delta S_{s/d}(\vec{Q})$, namely the difference of $S_{s/d}(\vec{Q})$ with and without the AFM fluctuations.

Here a clear peak is observed at $\vec{Q}_0 = (2\pi/\lambda, 2\pi/\lambda)$ where $\lambda \approx 8a/3$. Interestingly the d form factor CDW is stronger than the s-wave one. In the system studied ($L = 16$) this peak wavevector is consistent with that connecting a pair of hot spots displaced in the diagonal direction, namely $\vec{Q}_0 = (2\pi/3a, 2\pi/3a)$. However, disagreeing with experiments, the CDW wavevectors lie in the diagonal directions. This result agrees with previous approximate theoretical calculations involving hot spots[22, 23, 27]. The red dots in Fig. 3(c) show the dependence of $\Delta S_d(\vec{Q}_0)$ on $1/L$. The extrapolation to $L = \infty$ gives zero within errorbar hence suggesting there is no long-range CDW order. Given the fact that the ground state possesses SC long-range order this should not be a surprise because these two types of symmetry breaking compete with each other.

CDW correlation induced by both AFM and nematic fluctuations

The fact that the predicted directions of the CDW ordering wavevector are inconsistent with experiments makes us to suspect that AFM fluctuations alone is *insufficient* to account for the effective interaction. Motivated by the fact that nematicity has been observed in many cuprates[15–18], we add the nematic fluctuations to the
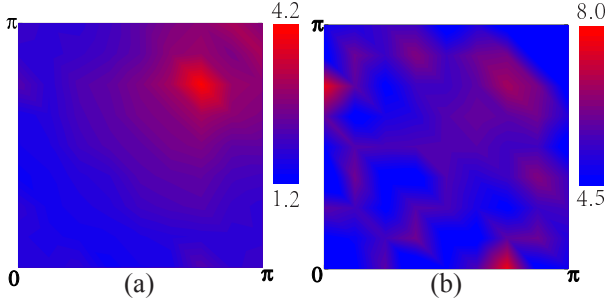
FIG. 4. (a) $\Delta S_d(\vec{Q})$ for $r_s = 0.5$ and $L = 16$ is plotted over the first quadrant of the Brillouin zone. The peak is situated around $\vec{Q} = (2\pi/3, 2\pi/3)$. (b) $\Delta S_d(\vec{Q})$ for $L = 16$, driven by both spin ($r_s = 0.5$) and nematic ($r_n = 0.5$) fluctuations. The strongest peaks are situated around $\vec{Q} = (2\pi/3, 0)$ and $(0, 2\pi/3)$.

effective action, which amounts to $S \rightarrow S + \Delta S$ where

$$\Delta S = \lambda_n \int_0^\beta d\tau \sum_i \chi_i \left[\psi_{ix}^\dagger \sigma_0 \psi_{ix} - \psi_{iy}^\dagger \sigma_0 \psi_{iy} \right] + S_n$$

$$S_n = \int_0^\beta d\tau \left\{ \frac{1}{2} \sum_i \frac{1}{c_n^2} |\partial_\tau \chi_i|^2 + \frac{1}{2} \sum_{\langle ij \rangle} |\chi_i - \chi_j|^2 \right.$$
$$\left. + \sum_i \left[\frac{r_n}{2} |\chi_i|^2 + \frac{u_n}{4} \chi_i^4 \right] \right\}. \tag{6}$$

The parameter that controls the strength of the nematic fluctuations in Eq. (6) is r_n. Large positive r_n causes the nematic order to become disordered. In Fig. 3(b) we plot $S_{s/d}(\vec{Q})$ for $L = 16$ after the inclusion of the nematic fluctuations. Here we choose $r_s = 0.5, r_n = 0.5$ which is on the disordered side of both the AFM and nematic phase transitions. The results show a d-wave bond CDW with wavevectors $\vec{Q} = (\pm 2\pi/\lambda, 0)$ and $(0, \pm 2\pi/\lambda)$ where $\lambda \approx 8a/3$, i.e., a stripe-like CDW, becomes the dominant charge density wave instability! The $\Delta S_d(\vec{Q})$ without and with the nematic fluctuations are plotted over the entire Brillouin zone in Fig. 4(a) and Fig. 4(b). These plots confirm the global maximum of $\Delta S_d(\vec{Q})$ in the whole Brillouin zone indeed locates at the previously described locations.

With the nematic fluctuations the CDW correlation is still short-ranged. This is shown by the red points of Fig. 3(c) which plots $\Delta S_d(\vec{Q}_0)$ as a function of $1/L$; again the extrapolation to the thermodynamic limit suggests there is no CDW long-range order. However in the presence of external translation symmetry breaking perturbations, such as quenched disorders, an actual CDW pattern can be induced even when there is no CDW long-range order. Such kind of patterns can be observed in an STM experiment. In Fig. 5(a), we show a static CDW pattern induced by the open boundary condition in the system of size $L = 16$. (The (r_s, r_n) used to generate this pattern is $(0.5, 0.5)$.) The CDW modulation wavevector
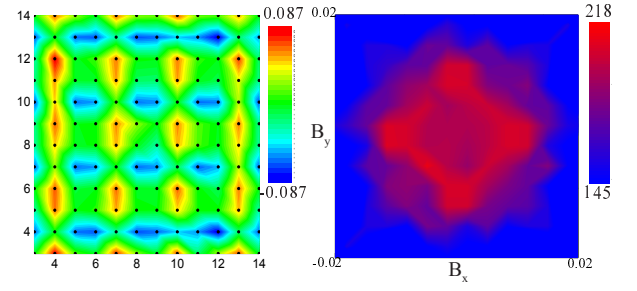

FIG. 5. (a) The d-wave bond CDW order parameter $\langle B_d(i) \rangle \equiv \langle \sum_{a=\pm\hat{x}} \psi_{i,x}^\dagger \sigma_0 \psi_{i+a,x} - \sum_{a=\pm\hat{y}} \psi_{i,y}^\dagger \sigma_0 \psi_{i+a,y} \rangle$ in a system of size $L = 16$ with open boundary conditions. Here σ_0 is the identity matrix in the spin space. The black dots represent the lattice sites. The pattern of bond CDW order parameter modulations obtained numerically is almost perfectly consistent with the expected modulations with $3a$ period. (b) The concurrence probability $P(B_x, B_y)$ in the QMC simulations is plotted as a function of B_x and B_y, where $B_{x/y}$ are the d-wave bond CDW order parameters associated with ordering wavevector $(2\pi/3, 0)$ and $(0, 2\pi/3)$, respectively. The system size in this computation is $L = 15$, and the parameters (r_s, r_n) used is $(0.5, 0.5)$.

is about $2\pi/3a$ agreeing with the result discussed earlier. In addition the d-wave nature of the bond CDW is transparent. Since the form factor for the CDW in electron doped cuprates has not been measured, this result is also a prediction.

Various approximate analytical calculations have been done on similar AFM effective models[22, 23, 27, 48, 49] as well as microscopic models [50] to address the origin of CDW instability in cuprate. Although some of them claim that AFM fluctuation can induce the CDW instability observed in cuprate experiments, systematical comparison of the CDW instabilities between wavevectors in horizontal and diagonal directions has not been done. In this work, we showed that although short-ranged CDW with ordering wavevector in the horizontal direction can be enhanced by pure AFM fluctuations, the dominant ordering wavevector actually lies in the diagonal direction. Only after we include the nematic fluctuations does the dominant ordering wavevector change to the horizontal direction. As the QMC simulation is unbiased and approximation-free, our results clearly demonstrate that pure AFM fluctuation is not enough to describe the CDW order in electron-doped cuprate.

For hole doped cuprates an open issue concerning the CDW is whether it is uni- or bi-directional. The answer relies on the sign of the quartic coupling between the horizontal and vertical CDW order parameters in the Ginzburg-Landau action. Since the quartic term only becomes significant when the magnitude of the order parameter is appreciable, it is difficult to answer this question by watching the induced CDW pattern in a system without the CDW long range order,

such as that in Fig. 5(a). However in a Monte-Carlo simulation we can employ the histogram method [43] to determine the concurrence probability $P(B_x, B_y)$ where $B_{x,y}$ are the CDW order parameters associated with $\vec{Q} = (\pm 2\pi/3a, 0)$ and $(0, \pm 2\pi/3a)$, respectively (see the details of histogram method in [41]). If the quartic coupling favors the uni-directional CDW, the peaks of P should appear on the horizontal and vertical axes of the (B_x, B_y) plane. Conversely if the quartic coupling favors the bi-directional CDW the peaks should appear along the diagonal direction. In Fig. 5(b) we plot P over the (B_x, B_y) plane. Four peaks on horizontal and vertical axes are seen, implying the quartic coupling term favors the uni-directional (stripe) CDW.

The effects of nematic fluctuation on pairing

Finally we return to the study of superconductivity. Specifically we study the effects of nematic fluctuation on the SC order. In Fig. 2(c), we plot the SC pair correlation at $\vec{x}_{\max}$ for L=14, with and without nematic fluctuations, as a function of r_s. The results show d-wave SC pairing correlations is enhanced in the presence of nematic fluctuations ($r_n = 0.5$). This result agrees with previous approximate theories[44–46]. In Supplementary Material III [41] we also show SC with mixed s- and d-wave symmetry can coexist with the nematic long-range ordered phase.

Concluding remarks

Our intrinsically-unbiased and numerically-exact QMC study of hot spot-based effective theory clearly indicates antiferromagnetic spin fluctuation alone does not lead to the CDW correlation recently observed in electron doped cuprates. When nematic fluctuation is added not only CDW with the correct ordering wavevectors is induced but also an enhanced d-wave superconducting long-range order is observed. Such effective theory predicts bond (rather than site) CDW with d-form factor just as in hole doped cuprates. This prediction should be testable by STM experiments in the future. We conclude with an effective action featuring the hot spots and both antiferromagnetic and nematic fluctuations as the low energy description of electron doped copper-oxide high temperature superconductors. We believe such effective action share many qualitative properties with that of the hole doped cuprates.

Acknowledgement

———————

[1] J.G. Bednorz and K.A. Müller, Z. Phys. B-Condensed Matter, **64**,189-193 (1986).

[2] J. M. Tranquada *et al.* Evidence for stripe correlations of spins and holes in copper oxide superconductors. Nature **375**, 561 (1995).

[3] T. Wu *et al.* Magnetic-field-induced charge-stripe order in the high-temperature superconductor $YBa_2Cu_3O_y$. Nature **477**, 191 (2011).

[4] A. Mesaros *et al.* Topological defects coupling smectic modulations to intra unit-cell nematicity in cuprates. Science **333**, 426 (2011).

[5] J. Chang, *et al.* Direct observation of competition between superconductivity and charge density wave order in $YBa_2Cu_3O_{6.67}$. Nature Physics **8**, 871-876 (2012).

[6] G. Ghiringhelli, *et al.* Long-Range Incommensurate Charge Fluctuations in $(Y,Nd)Ba_2Cu_3O_{6+x}$. Science **337**, 821-825 (2012).

[7] K. Fujita *et al.* Direct phase-sensitive identification of a d-form factor density wave in underdoped cuprates. PNAS **111**, E3026-E3032 (2014).

[8] R. Comin *et al.* Charge order driven by Fermi-arc instability in $Bi_2Sr_{2-x}La_xCuO_{6+\delta}$. Science **343**, 390-392 (2014).

[9] W. Tabis *et al.* Charge order and its connection with Fermi-liquid charge transport in a pristine high-T_c cuprate. Nat. Commun. **5**, 5875 (2014).

[10] M. Hashimoto *et al.* Direct observation of bulk charge modulations in optimally doped $Bi_{1.5}Pb_{0.6}Sr_{1.54}CaCu_2O_{8+\delta}$. Phys. Rev. B **89**, 220511 (2014).

[11] R. Comin *et al.* Symmetry of charge order in cuprates. Nature Materials **14**, 796 (2015).

[12] E. H. da Silva Neto *et al.* Charge ordering in the electron-doped superconductor $Nd_{2-x}Ce_xCuO_4$. Science **347**, 282 (2015).

[13] E. H. da Silva Neto *et al.* Doping-dependent charge order correlations in electron-doped cuprates. Science Advance **2**, e1600782 (2016).

[14] S. Gerber *et al.* Three-dimensional charge density wave order in $YBa_2Cu_3O_{6.67}$ at high magnetic fields. Science **350**, 949 (2015).

[15] Y. Ando *et al.* Electrical resistivity anisotropy from self-organized one dimensionality in high-temperature superconductors. Phys. Rev. Lett. **88**, 137005 (2002).

[16] V. Hinkov *et al.* Electronic liquid crystal state in the high-temperature superconductor $YBa_2Cu_3O_{6.45}$. Science **319**, 597-600 (2008).

[17] M. J. Lawler *et al.* Intra-unit-cell electronic nematicity of the high-T_c copper-oxide pseudogap states. Nature **466**, 347-351(2010).

[18] R. Daou *et al.* Broken rotational symmetry in the pseudogap phase of a high-Tc superconductor. Nature **463**, 519 (2010).

[19] E. Fradkin and S. A. Kivelson. High-temperature superconductivity: Ineluctable complexity. Nature Physics **8**, 865 (2012).

[20] J. C. S. Davis and D.-H. Lee. Concepts relating magnetic interactions, intertwined electronic orders, and strong-

ly correlated superconductivity. PNAS **110**, 17623-17630 (2013).

[21] E. Fradkin, S. A. Kivelson, and J. M. Tranquada. How to detect fluctuating stripes in the high-temperature superconductors. Rev. Mod. Phys. **87**, 457 (2015).

[22] K. B. Efetov, H. Meier and C. Pepin. Pseudogap state near a quantum critical point. Nature Physics **9**, 442 (2013).

[23] S. Sachdev and R. La Placa. Bond order in two-dimensional metals with antiferromagnetic exchange interactions. Phys. Rev. Lett. **111**, 027202 (2013).

[24] D. Chowdhury and S. Sachdev. Feedback of superconducting fluctuations on charge order in the underdoped cuprates. Phys. Rev. B **90**, 134516 (2014).

[25] D. Chowdhury and S. Sachdev. Density-wave instabilities of fractionalized Fermi liquids. Phys. Rev. B **90**, 245136 (2014).

[26] Y. Wang and A. Chubukov. Superconducting and charge-density-wave orders in the spin-fermion model: a comparative analysis. Phys. Rev. B **91**, 195113 (2015).

[27] Y. Wang and A. Chubukov. Charge-density-wave order with momentum$(2Q,0)$ and$(0,2Q)$ within the spin-fermion model: Continuous and discrete symmetry breaking, preemptive composite order, and relation to pseudogap in hole-doped cuprates. Phys. Rev. B **90**, 035149.

[28] Armitage, N. P., *et al.*. Superconducting Gap Anisotropy in $Nd_{1.85}Ce_{0.15}CuO_4$: Results from Photoemission. Phys. Rev. Lett. 87, 147003 (2001).

[29] H. Matsui *et al.*. Evolution of the pseudogap across the magnet-superconductor phase boundary of $Nd_{2x}Ce_xCuO_4$ Phys. Rev. B **75**, 224514 (2007).

[30] N.P. Armitage, P. Fournier and R.L. Greene. Progress and perspectives on electron-doped cuprates. Rev. Mod. Phys. **82**, 2421 (2010).

[31] G. Blumberg *et al.*. Nonmonotonic $d_{x^2y^2}$ Superconducting Order Parameter in $Nd_{2x}Ce_xCuO_4$. Phys. Rev. Lett. **88**, 107002 (2002).

[32] H. Matsui *et al.*. Superconducting Gap in the Electron-Doped High-Tc Superconductor $Pr_{0.89}LaCe_{0.11}CuO_4$. Phys. Rev. Lett. **95**, 017003 (2005).

[33] A. Abanov and A. V. Chubukov. Spin-fermion model near the quantum critical point: one-loop renormalization group results. Phys. Rev. Lett. **84**, 5608 (2000).

[34] A. Abanov and A. Chubukov. Anomalous scaling at the quantum critical point in itinerant antiferromagnets. Phys. Rev. Lett. **93**, 255702 (2004).

[35] M. A. Metlitski and S. Sachdev. Quantum phase transitions of metals in two spatial dimensions. II. Spin density wave order. Phys. Rev. B **82**, 075128 (2010).

[36] S. A. Hartnoll, D. M. Hofman, M. A. Metlitski, and S. Sachdev. Quantum critical response at the onset of spin-density-wave order in two-dimensional metals. Phys. Rev. B **84**, 125115 (2011).

[37] E. Berg, M. A. Metlitski, and S. Sachdev. Sign-Problem-Free Quantum Monte Carlo of the Onset of Antiferromagnetism in Metals. Science **338**, 1606 (2012).

[38] S. Sorella, S. Baroni, R. Car and M. Parrinello. A novel technique for the simulation of interacting fermion systems. Europhys. Lett. **8**, 663 (1989).

[39] S. R. White, D. J. Scalapino, R. L. Sugar, E. Y. Loh, J. E. Gubernatis and R. T. Scalettar. Numerical study of the two-dimensional Hubbard model. Phys. Rev. B, **40**, 506 (1989).

[40] F. F. Assaad and H. G. Evertz. Computational Many-Particle Physics, 277-356 (Lect. Notes Phys. 739, Springer, 2008).

[41] See Supplemental Materials for the details.

[42] K. Binder. Finite size scaling analysis of Ising model block distribution functions. Zeitschrift fur Physik B Condensed Matter **43**, 119-140 (1981).

[43] A. F. Albuquerque *et al*. Phase diagram of a frustrated quantum antiferromagnet on the honeycomb lattice: Magnetic order versus valence-bond crystal formation. Phys. Rev. B, **84**, 024406 (2011).

[44] T.A Maier and D.J. Scalapino. Pairing interaction near a nematic quantum critical point of a three-band CuO_2 model. Phys. Rev. B **90**, 174510 (2014).

[45] M. A. Metlitski, D. F. Mross, S. Sachdev, and T. Senthil. Cooper pairing in non-Fermi liquids. Phys. Rev. B **91**, 115111 (2015).

[46] S. Lederer, Y. Schattner, E. Berg, and S. A. Kivelson. Enhancement of superconductivity near a nematic quantum critical point. Phys. Rev. Lett. **114**, 097001 (2015).

[47] Y. Schattner, M. H. Gerlach, S. Trebst, and E. Berg. Competing Orders in a Nearly Antiferromagnetic Metal, Phys. Rev. Lett. **117**, 097002 (2016).

[48] Y. Yamakawa and H. Kontani, Spin-Fluctuation-Driven Nematic Charge-Density Wave in Cuprate Superconductors: Impact of Aslamazov-Larkin Vertex Corrections, Phys. Rev. Lett. **114**, 257001 (2015).

[49] M. Tsuchiizu, Y. Yamakawa, and H. Kontani, p-orbital density wave with d symmetry in high-Tc cuprate superconductors predicted by renormalization-group + constrained RPA theory, Phys. Rev. B, **93**,155148 (2015).

[50] H. Yamase, M. Bejas, A. Greco, *d*-wave bond-order charge excitations in electron-doped cuprates, Europhys. Lett. **111**, 57005 (2015).